Supplement of Earth Surf. Dynam., 10, 705–722, 2022
https://doi.org/10.5194/esurf-10-705-2022-supplement

Earth Surface Dynamics
Open Access

Supplement of

The imprint of erosion by glacial lake outburst floods in the topography of central Himalayan rivers

Maxwell P. Dahlquist and A. Joshua West

Correspondence to: Maxwell P. Dahlquist (mpdahlqu@sewanee.edu)

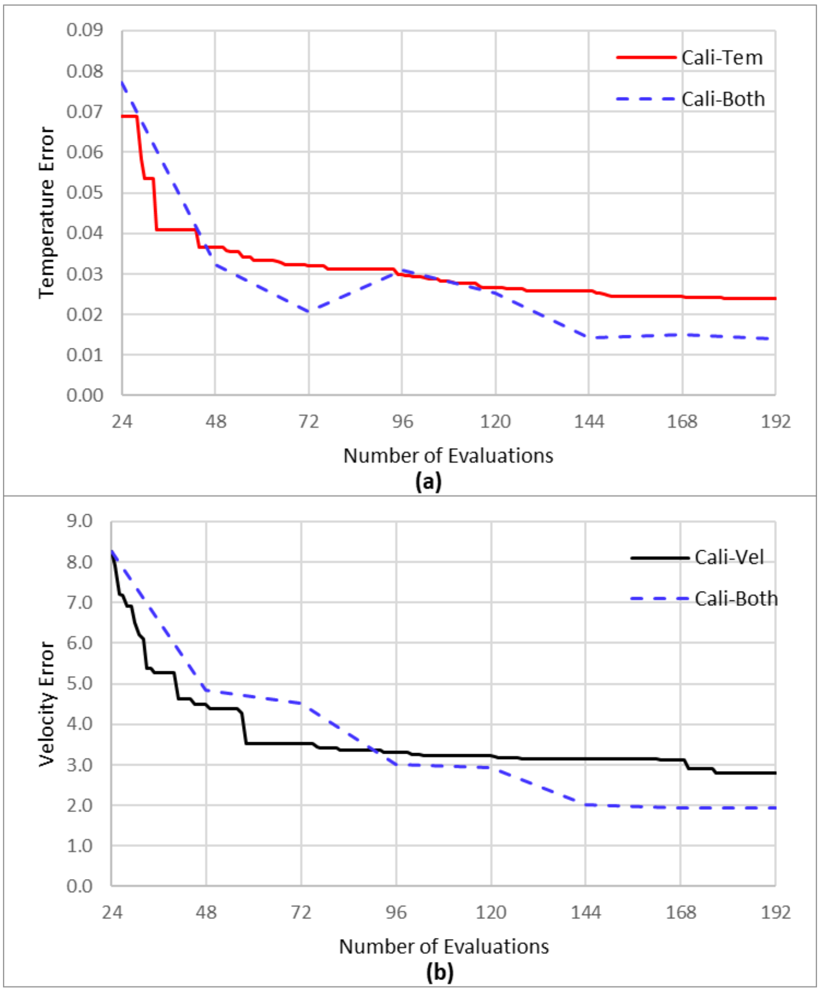

Figure S1. Calibration progress plot of PODS in Cali-Tem, Cali-Vel, and Cali-Both scenarios. The best solution found so far in average of three trials is plotted with the number of evaluations. Calibration progress of PODS in the Cali-Tem scenario is plotted in (a), where the temperature error ($f_{Tem}(\boldsymbol{X})$in Eq. (7)) of the best solution found so far is plotted. Calibration progress of the Cali-Vel scenario is plotted in (b), where the velocity error ($f_{\overline{Vel}}(\boldsymbol{X})$ in Eq. (10)) is plotted. The calibration progress of PODS in the Cali-Both scenario is plotted in (a) and (b) in terms of temperature error and velocity error, respectively, of the best solution found so far based on Eq. (12).

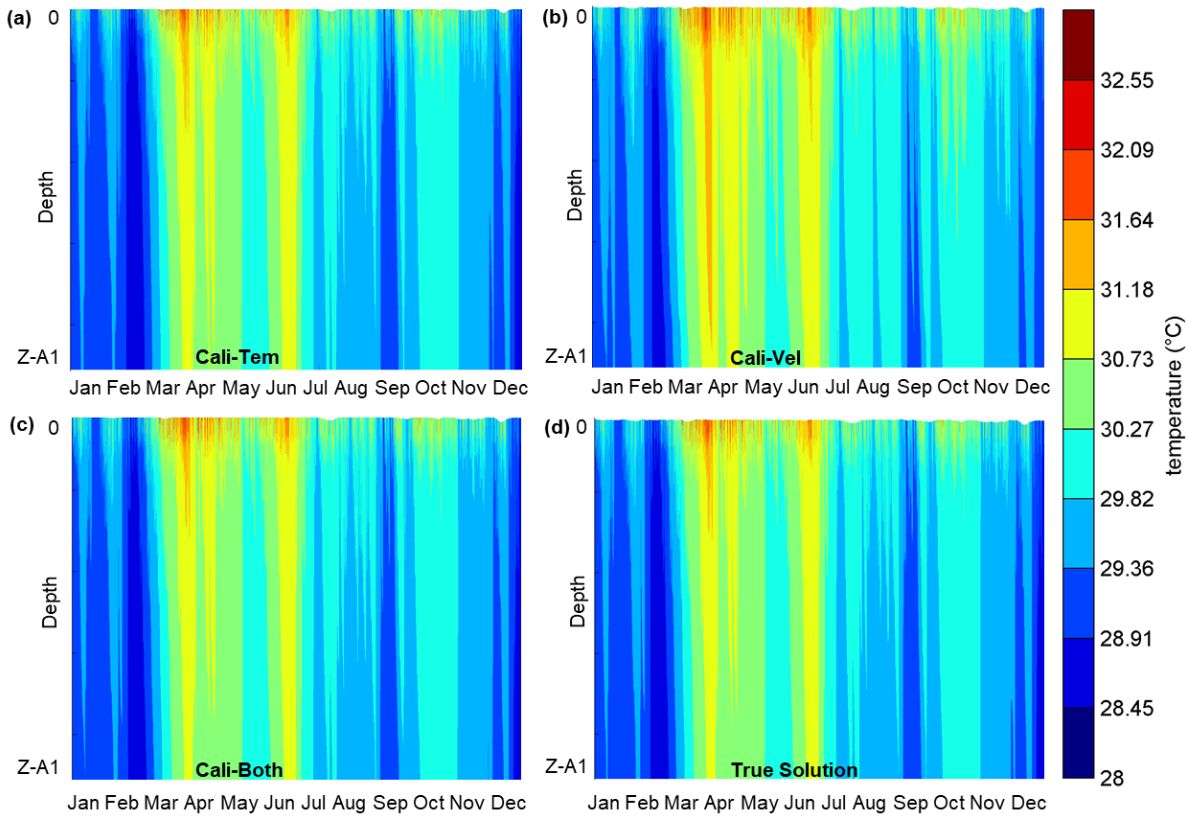

Figure S2. The change of vertical temperature profiles at STN. A1 with the change of time. The result of three calibration scenarios (Cali-Tem, Cali-Vel, and Cali-Both) and the True solution is plotted.

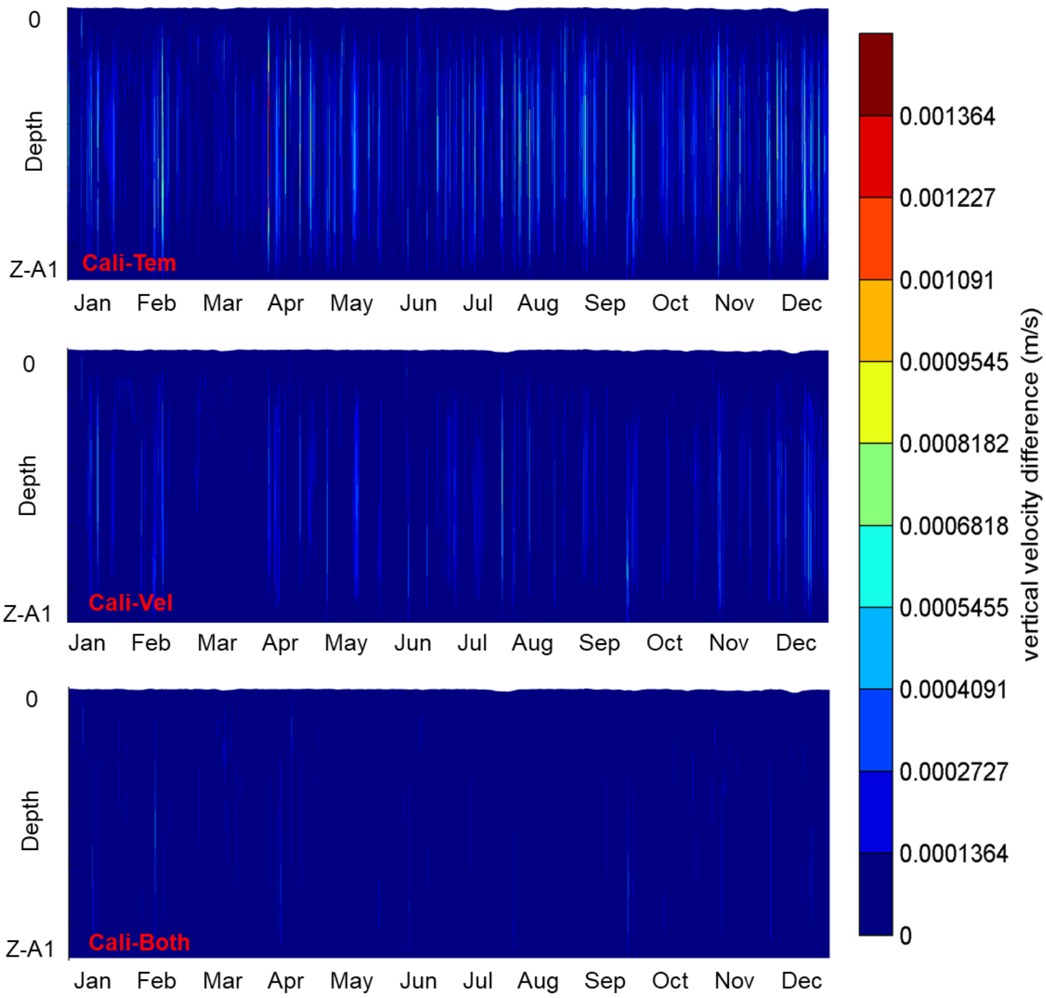

Figure S3. The absolute vertical velocity error at STN. A1 between the calibrated results (in the Cali-Tem, Cali-Vel, and Cali-Both scenarios) and the true solution. The change of absolute vertical velocity error is plotted with the change of time.

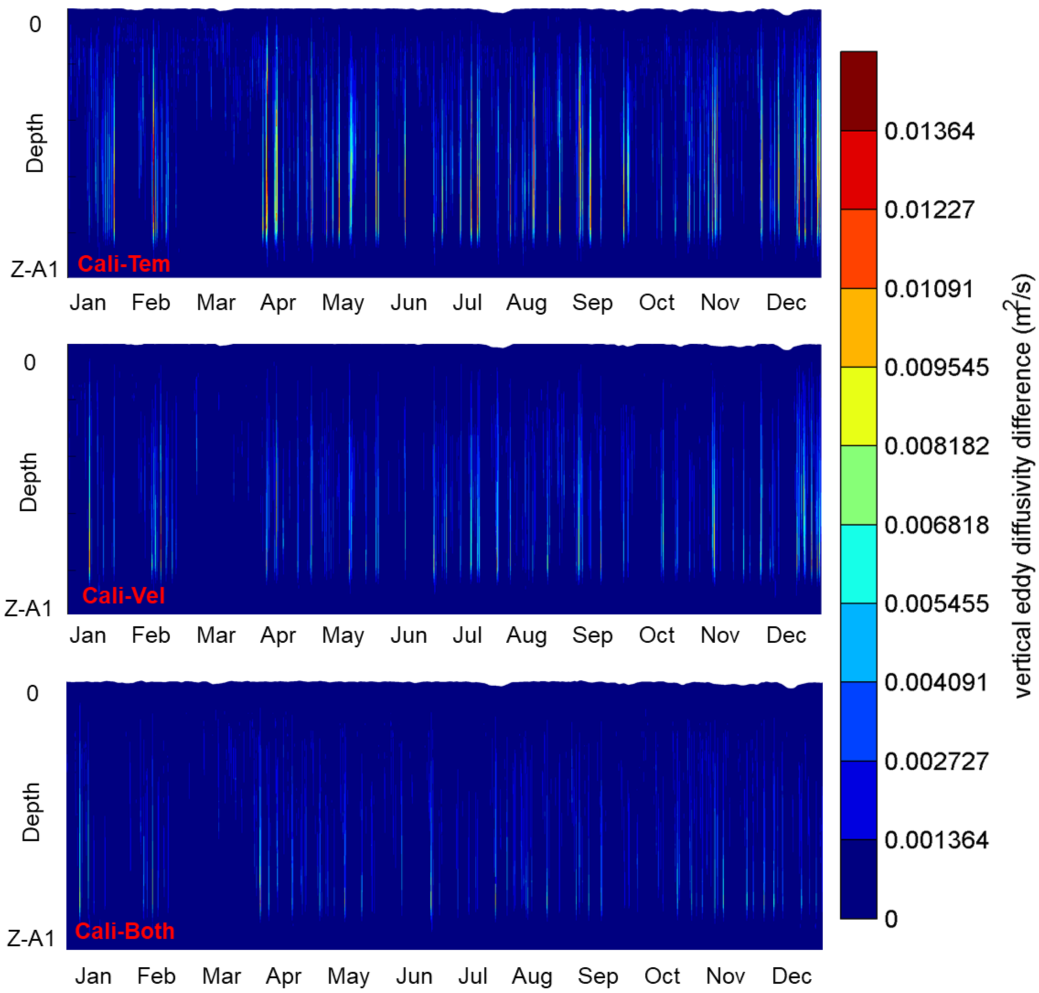

Figure S4. The absolute vertical eddy diffusivity error at STN. A1 between the calibrated results (in the Cali-Tem, Cali-Vel, and Cali-Both scenarios) and the true solution. The change of absolute vertical eddy diffusivity error is plotted with the change of time.

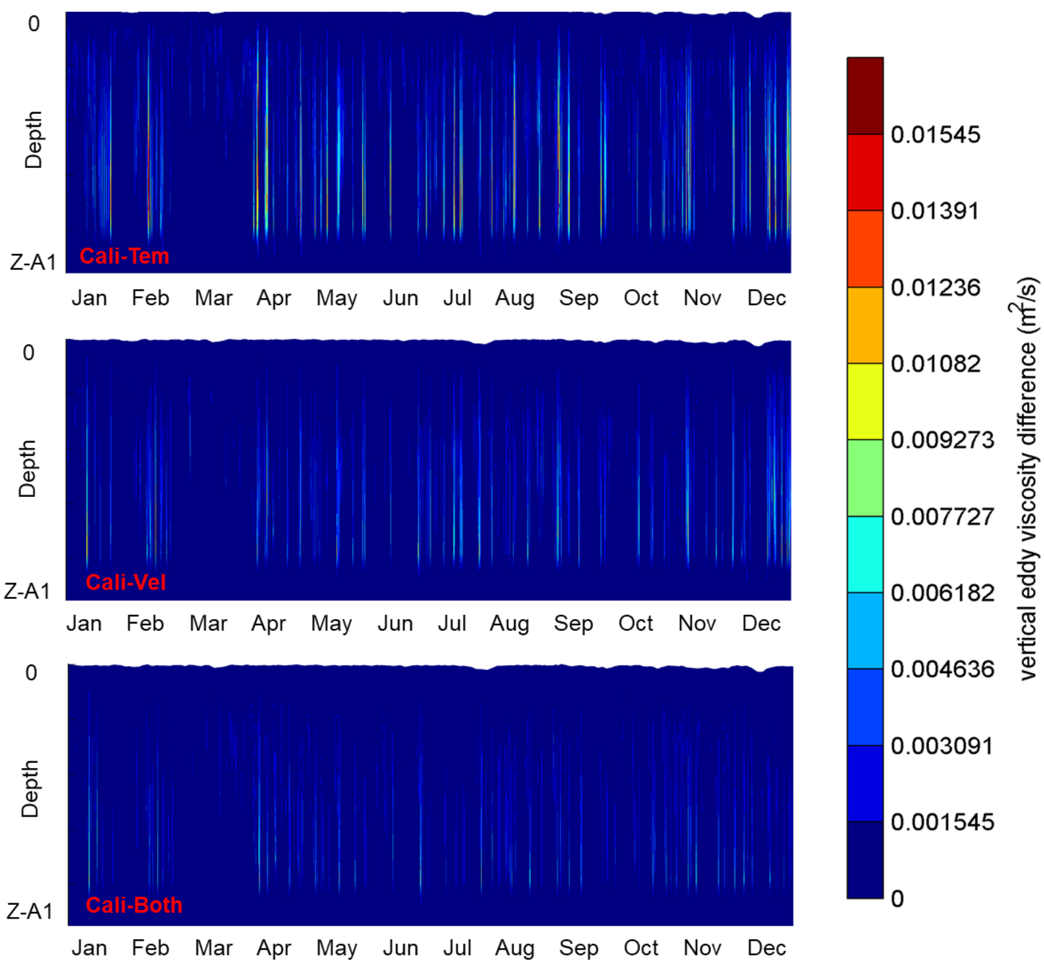

Figure S5. The absolute vertical eddy viscosity error at STN. A1 between the calibrated results (in the Cali-Tem, Cali-Vel, and Cali-Both scenarios) and the true solution. The change of absolute vertical viscosity error is plotted with the change of time.

Table S1. The composite error of each variable and the corresponding parameter configuration of the selected optional solution obtained via PODS in three calibration scenarios (Cali-Tem, Cali-Vel and Cali-Both). True solution ($\boldsymbol{X}^R$) defined in Table 2 and an initial uncalibrated solution are given for reference. The parameter symbols are defined in Table 2.

		True Solution ($\boldsymbol{X}^R$)	Cali-Tem	Cali-Vel	Cali-Both	Uncalibrated
Composite error of each variable[1]	$f_{Tem}(\boldsymbol{X})$	0	0.0202	0.0601	0.0108	0.1107
	$f_{\overrightarrow{Vel}}(\boldsymbol{X})$	0	5.1945	2.7390	1.8006	10.3358
Computed Parameter Vector ($\boldsymbol{X}$*)	$\boldsymbol{v_H^{back}}$ (m^2/s)	0.5	0.7107	0.5084	0.4516	0.55
	$\boldsymbol{D_H^{back}}$ (m^2/s)	0.5	0.1930	0.8427	0.4562	0.55
	$\boldsymbol{v_V^{back}}$ (m^2/s)	5.00E-05	3.96E-04	3.40E-05	3.00E-05	2.50E-03
	$\boldsymbol{D_V^{back}}$ (m^2/s)	5.00E-05	1.12E-04	6.08E-06	2.98E-05	2.50E-03
	$\boldsymbol{L_{oz}}$ (m)	0.015	0.0110	0.0490	0.0340	0.025
	$\boldsymbol{H_{Secchi}}$ (m)	1	0.5902	1.4147	1.1358	1.05
	$\boldsymbol{c_e}$ (-)	0.0013	0.0017	0.0013	0.0011	0.0015
	$\boldsymbol{c_H}$ (-)	0.0013	0.0013	0.0012	0.0013	0.0015
	$\boldsymbol{n}$ ($m^{-1/3}s$)	0.022	0.0229	0.0209	0.0243	0.025

[1]Smaller variable errors ($f_{Tem}(\boldsymbol{X})$ (see Eq. (7)) and $f_{\overrightarrow{Vel}}(\boldsymbol{X})$ (see Eq. (10))) are better, and the variable errors of the true solution $\boldsymbol{X}^R$ are zero (for both $f_{Tem}(\boldsymbol{X})$ and $f_{\overrightarrow{Vel}}(\boldsymbol{X})$).